

RSC Advances

Accepted Manuscript



This article can be cited before page numbers have been issued, to do this please use: V. Mahdavi and A. Monajemi, *RSC Adv.*, 2016, DOI: 10.1039/C6RA24614A.



This is an Accepted Manuscript, which has been through the Royal Society of Chemistry peer review process and has been accepted for publication.

Accepted Manuscripts are published online shortly after acceptance, before technical editing, formatting and proof reading. Using this free service, authors can make their results available to the community, in citable form, before we publish the edited article. We will replace this Accepted Manuscript with the edited and formatted Advance Article as soon as it is available.

You can find more information about Accepted Manuscripts in the [author guidelines](#).

Please note that technical editing may introduce minor changes to the text and/or graphics, which may alter content. The journal's standard [Terms & Conditions](#) and the ethical guidelines, outlined in our [author and reviewer resource centre](#), still apply. In no event shall the Royal Society of Chemistry be held responsible for any errors or omissions in this Accepted Manuscript or any consequences arising from the use of any information it contains.

Gas Phase Dehydration of Glycerol Catalyzed by Gamma Al₂O₃ Supported V₂O₅: A Statistical Approach for Simultaneous Optimization

Vahid Mahdavi* and Ali Monajemi

*Department of Chemistry, Surface Chemistry and Catalysis Division, Faculty of Sciences,
Arak University, Arak 38156-8-8349, Iran*

Corresponding author; Vahid Mahdavi

Department of Chemistry

Faculty of Sciences

Arak University

Arak 38156-8-8349

Iran

Fax: +98 863 4173406

E-mail: v-mahdavi@araku.ac.ir

Abstract

Selective gas-phase dehydration of glycerol to acrolein over $V_2O_5/\gamma-Al_2O_3$ catalysts was investigated. The catalysts with various V_2O_5 loading were facilely synthesized by impregnation method. The prepared catalysts were characterized by several techniques such as scanning electron microscopy (SEM), temperature-programmed desorption of NH_3 (TPD- NH_3), Temperature programmed reduction (H_2 -TPR), Fourier transform infrared spectroscopy (FT-IR), Brunauer–Emmett–Teller (BET) and X-ray diffraction (XRD). The effects of V_2O_5 loading (5–25 wt %), gas hourly space velocity (G.H.S.V) of O_2/N_2 (120–540 h^{-1}) and reaction temperature (250–320°C) on yield of acrolein were studied by Box–Behnken design. The influence of independent factors and their quadratic interactions were examined by means of the Analysis of Variance (ANOVA). Present results indicate that temperature has a different effect on the conversion and selectivity of acrolein. The catalyst with 14.80wt% of V_2O_5 loading, G.H.S.V of 268.60 h^{-1} and reaction temperature of 286.35°C produced maximum yield of acrolein (73.05 %). The analysis revealed that the predicted results agree well with the experimental data (12.5wt% loading of V_2O_5 on $\gamma-Al_2O_3$, G.H.S.V of the carrier gas = 330 h^{-1} and reaction temperature of 285°C with 68.31% yield).

Keywords: Gas phase dehydration; Glycerol; Acrolein; $V_2O_5/\gamma-Al_2O_3$; Box-Behnken design

1. Introduction

Nowadays, the investigation of biomass-derivable feedstock as a starting material for production of chemical materials is an attractive research topic [1, 2]. Because of continuous availability in a large amount from the biodiesel production process, glycerol has gained too much attention [3]. Depletion of fossil fuels and the impacts of global warming have also been identified as critical problem and the utilization of biomass-derivable feedstock such as catalytic dehydration of glycerol to acrolein can be an efficient way to overcome this challenge. Therefore, it is essential to gain cost-effective ways of utilizing glycerol that will be beneficial for both biodiesel manufacturing and environment. Acrolein is currently produced by oxidation of propylene over Bi-Mo catalysts [4]. It is usually converted to acrylic acid, which is widely used in adhesives, plastics, fibers, polymer dispersions and other chemical intermediates. The most significant direct application of acrolein is as a herbicide to control the growth of aquatic plants [3]. Many studies have been reported on the dehydration of glycerol and confirmed that the selectivity to acrolein is related to the presence of Brønsted acid sites [1, 5]. Therefore it is crucial to understand and find the best combination of parameters such as: reaction temperature, gas hourly space velocity and catalyst textural for improving the selectivity of acrolein in this reaction. Researchers have applied various experimental and statistical techniques to optimize and improve the process parameters. Using a one factor at a time optimization method is an intricate approach to evaluate the effects of different variables on an experimental outcome. The application of modeling tools such as response surface methodology (RSM) can extremely reduce the need for a large number of laboratory tests and associated costs. The catalytic developments in the reaction dehydration of glycerol to acrolein has widely been investigated in the gas phase over

solid acid catalysts such as heteropoly acids [6, 7] metal oxides, [8, 9], supported zeolites [10, 11]. In general, dehydration of glycerol to acrolein in the gas phase has higher yield than in the liquid phase even when using the same type of solid catalyst [12]. Talebian et al. reported gas-phase glycerol dehydration to acrolein over supported silicotungstic acid catalyst and used Central composite design (CCD) to evaluate the interactions on reaction conversion [2]. Dubois et al. used $\text{WO}_3\text{-ZrO}_2$ catalysts and obtained high selectivity of acrolein (60 %) for dehydration of glycerol [13]. Regardless of the reaction phase, the strength and nature of the acid sites is a critical factor in selective production of acrolein from glycerol, as well as the influence of the morphology and textural properties of the solids [1, 14]. Wang et al. reported dehydration of glycerol over VPO oxides catalysts because of their mild acid-basic properties and added molecular oxygen into reaction in order to reduce side reactions and avoid coke formation [15]. Finally, they concluded that vanadyl hydrogen phosphate hemihydrate $\text{VOHPO}_4 \cdot 0.5\text{H}_2\text{O}$ has the best performance with 66% selectivity for acrolein at 100% conversion of glycerol [16]. Kamiya et al. reported that the total amount of Brønsted and Lewis acid sites of VPO catalyst with different preparation methods is an important parameter in the yield of acrolein [17]. Cecilia et al. prepared a series of catalysts, based on vanadium and vanadium-phosphorous containing Zr-SBA-15 and concluded that dehydration reaction of glycerol to acrolein could take place inside the meso channels for vanadium based catalysts [18]. Wang et al. reported a new route for selective and efficient glycerol dehydration to acrolein and found that Brønsted and Lewis acid sites significantly improved the yield of acrolein [5]. Alhanash et al. suggested two reaction pathways based on the nature of acid sites and reported that dehydration of primary hydroxyl groups of glycerol at Lewis acid sites enhance the acetol production but dehydration of the internal secondary and terminal

primary hydroxyl groups both occurring at Brønsted acid sites and greatly enhanced the production of acrolein [19].

Chierigato et al. synthesized bicomponent W-Mo, tricomponent W-Mo-V oxides, VO-WO_x and V-Co-AlPO₄ as a new class of catalysts for the one-pot conversion of glycerol to acrylic acid and obtained high yields of acrylic acid (up to 51 %) [20, 21]. Souza et al. synthesized NbV, NbMo and pure Nb catalysts and used Box-Behnken design (BBD) to evaluate the metal doping, solvent and effect of temperature in the oxidation of glycerol to cyclic ethers [22]. Arkema Company patented a way to reduce side products through addition of oxygen during the dehydration reaction and obstruct catalyst deactivation base on acidic materials such as ZrO₂, SO₄, WO₃ and Al₂O₃ [23]. Omata et al. synthesized W-Nb-O catalysts by hydrothermal method and achieved high yield of acrolein in gas phase glycerol dehydration in the presence of these catalysts, water and oxygen [24]. But there have been a few reports on the favorable outcome optimization of RSM in glycerol conversion processes and dehydration of glycerol to acrolein. These researches had different problems such as large amounts of by-products, severe coke formation, low thermal stability and harsh reaction conditions. These problems must be solved in order to gain economical and continuous industrial production.

In this work, for the first time, a novel V₂O₅/Al₂O₃ catalyst with different loading of V₂O₅ was prepared by impregnation method. Since V₂O₅ have low surface areas so γ -Al₂O₃ nanoparticle was added as the second component to the catalyst in order to increase the surface area. This causes good dispersion of vanadium particles on the support surface without aggregation and also can affect the relative strength of acid sites. The influence of the preparation condition, such as loading of V₂O₅ supported on γ -Al₂O₃ (B) and operation conditions such as reaction temperature (A) and Gas hourly space velocity (G.H.S.V) (C) on the activity of the catalyst for acrolein yield were investigated. The

optimization of the dehydration reaction was carried out using response surface methodology (RSM). The relationships between the glycerol conversion and reaction parameters (factors) were evaluated to determine the optimum conditions for acrolein production. Scanning electron microscopy (SEM), Fourier transform infrared (FTIR) spectra of adsorbed pyridine, Brunauer–Emmett–Teller (BET), powder X-ray diffraction (XRD), temperature-programmed desorption of NH_3 (TPD- NH_3) and H_2 -TPR (Temperature programmed reduction) were employed to characterize the texture and structure of the catalysts.

2. Experimental

2.1. Materials

All materials were of commercial reagent grade. V_2O_5 (99.6% Alfa Aesar), Oxalic acid (99% Aldrich), Glycerol (purity >99%), Aluminum nitrate ($\text{Al}(\text{NO}_3)_3 \cdot 9\text{H}_2\text{O}$, 99% Merck), Sodium carbonate (Na_2CO_3 , 99.5%Merck) and deionized water were used as received without further purification. Gases employed were N_2 (99.9999%, Air Liquid) and dry air (99.99%, 20 wt% O_2/N_2).

2.2. Catalyst preparation

2.2.1. Preparation of Nano $\gamma\text{-Al}_2\text{O}_3$ powder

Nano-sized porous gamma alumina was synthesized according to a literature procedure [25]. Initially, 200 mL water was heated to 65°C in a 2 liter round bottomed double capped flask. Aluminum nitrate (0.05M) and sodium carbonate (0.075M) solutions were prepared by dissolving 18.75 g and 7.96 g in 250 mL of deionized water respectively and then added (drop by drop from two separate burettes) to 200 mL deionized Water. The gel was kept under vigorous stirring at 65 °C for 8 h to precipitate Al cations in the form of hydroxides and then aged for an additional 1 h. After vacuum filtration, the solid was

washed with distilled water and dried at room temperature for 1 day then was calcined in a programmable muffle furnace at 600 °C for 5 h in air with heating rate of 2 °C.min⁻¹ to produce γ -Al₂O₃ powders. The surface area of prepared γ -Al₂O₃ was 230 m².g⁻¹.

2.2.2. Preparation of the nano V₂O₅ and nano V₂O₅/ γ -Al₂O₃

In the first, V₂O₅ (9.09 g, 0.5 mol) and H₂C₂O₄ (13.50 g, 1.5 mol) in a stoichiometric ratio of 1 : 3 were dissolved to 100 mL distilled water under active stirring (800 RPM) at room temperature until the color of the solution changed from yellow to blue. The resulting solution was introduced into a 200 cm³ Teflon-lined stainless steel autoclave and submitted to a hydrothermal treatment at 250 °C for 24 h. The solid was separated by filtration, dried at 80 °C and then calcined in the furnace at 400 °C in air for 2 h [26] and finally labeled as nano V₂O₅. The V₂O₅/ γ -Al₂O₃ catalysts containing V₂O₅ with 5, 10, 15, and 20 wt% were prepared by impregnation method as described in [27]. In a typical synthesis, 1.0 g of calcined and out gassed γ -Al₂O₃ was impregnated with certain concentration of vanadyl oxalate solution. Above solution was prepared by mixing vanadium pentoxide with desire amounts of oxalic acid. The wet solid was then dried at 120 °C over night under vacuum and calcined in air under static conditions at 600 °C for 5 h. Finally, the obtained samples were crushed and sieved to obtain catalyst particle size of 0.077–0.300 mm.

2.3. Catalyst characterization

The structure of these samples was studied by X-ray diffraction (XRD) experiments. A Philips model PW 1800 diffractometer with Cu K α (λ = 0.15406 nm) radiation and Ni filter operating at 40 kV and 10 mA in the 2 θ range of 10–80° at a scanning rate of 4° .min⁻¹ was used to collect the X-ray data. Scanning electron microscopy (SEM) images were obtained with a Philips XL30 instrument. The specific surface areas were measured at -196 °C using the N₂ adsorption/desorption by the Brunauer–Emmett–Teller (BET) method

on a Micromeritics ASAP 2010 instrument. The pore size and average pore volume were calculated using the Barrett–Joyner–Halenda (BJH) method. The samples were degassed at 200°C for 8 h to remove impurities and physisorbed water prior to surface area measurements. Fourier transform infrared (FTIR) spectra of adsorbed pyridine were recorded on a Shimadzu 8300 spectrometer. The samples (10 mg) were activated at 400 °C under a vacuum of 1.33×10^{-3} Pa for 3h, followed by adsorption of purified pyridine vapor at room temperature for 30 min. After this step, the samples were evacuated at 100 °C and the pyridine -IR spectra were recorded. NH₃-TPD (ammonia temperature-programmed desorption) and H₂-TPR (Temperature programmed reduction) spectra were recorded on a Micromeritics Autochem 2920 chemisorption analyzer. The samples were pretreated by passage of high purity helium (50 mL.min⁻¹) at 220 °C for 1 h, then saturated with high purity anhydrous ammonia at 100 °C for 30-40 min and subsequently flushed at the same temperature for 30 min to remove physisorbed NH₃. TPD analysis was carried out from 50 to 600 °C at a heating rate of 10°C.min⁻¹. The amount of NH₃ consumed was monitored by using a thermal conductivity detector (TCD). TPR analysis was carried out from 50 to 850 °C with gaseous mixture of 10% H₂/Ar at a heating rate of 10 °C/min and total gases flow rate of 50 ml/min. The H₂ consumption was monitored by a calibrated thermal conductivity detector (TCD). Thermogravimetric- differential thermal analysis (TG-DTA) of the used catalyst (after 3 and 9 h) were performed with a Shimadzu TGA-51 thermogravimetric analyzer. The samples were heated from room temperature to 800°C, at a heating rate of 10°C/min, under a 100 mL.min⁻¹ flow of dry air.

2.4. Experimental design and catalytic reaction

In this study, the Box–Behnken design of experiment was employed to find the optimal conditions for gas phase dehydration of glycerol (GLY) and acrolein (ACR) production. The effects of temperature (A), V₂O₅ loading on the support (B) and G.H.S.V (C) were

investigated. The conversion of glycerol aqueous solution (GLY Conv %), acrolein selectivity (ACR Sele %) and yield (%) were calculated in the final reaction mixture according to the following equations:

$$\text{Glycerol conversion (\%)} = (\text{Moles of glycerol reacted} / \text{Moles of glycerol in the feed}) \times 100 \quad (1)$$

$$\text{Product selectivity (\%)} = (\text{Moles of carbon in a product defined} / \text{Mole of carbon in glycerol reacted}) \times 100 \quad (2)$$

$$\text{Product yield (\%)} = (\text{Conversion of glycerol} \times \text{Selectivity of acrolein}) / 100 \quad (3)$$

Glycerol dehydration reactions were conducted at atmospheric pressure in a vertical stainless steel reactor of 50 cm length and 0.9 cm internal diameter. The experimental setup is shown schematically in Fig. 1. A mixture of 5.0 g catalyst and 3.0 g corundum (50–70 mesh) was loaded in the middle section of the reactor, with quartz wool packed in both ends and was pretreated at 300 °C in G.H.S.V of 120 mL.h⁻¹ (dry air 20% O₂/N₂ was used as carrier gas) for 1 h before the reaction. The dry air was controlled by a Brooks mass flow controller. The reaction temperature was monitored by three thermocouples (TC.1-3) inserted into the middle of the catalyst. Aqueous glycerol (30%, w/w) was fed at a speed of 1 mL.h⁻¹ by a HPLC pump. The composition of fed gas was N₂:O₂:H₂O: glycerol, equal to 13.5:3:12:1 in molar ratio. After 3 h, reaction products were collected in an ice-water cold trap and n-butanol was added as internal standard. Products were quickly analyzed by Varian Star 3400 gas chromatograph equipped with a 10 wt. % FFAP/ChromosorbW-AW column (2 mm i.d., 2.5 m long) and FID detector. The main products identified by GC analysis were acrolein, acetol, allyl alcohol and acetaldehyde. The mass balance was determined and an acceptable carbon balance (>85%) was achieved for each trap. Besides, some chromatographic signals in lower quantities have not been identified. Glycerol conversion, selectivity and yield were calculated by Eqs. 1, 2, 3 respectively.

2.5. Response surface exploration

Several preliminary tests have been performed to evaluate the effect of parameters on glycerol conversion and acrolein selectivity over $V_2O_5/\gamma-Al_2O_3$ catalysts. Reaction temperature (A), V_2O_5 loading on support (B) and gas hourly speed velocity (G.H.S.V) (C) were regarded as most significant factors. In order to investigate the optimum levels of those variables and to study their relation, Box–Behnken experimental design was found to be more suitable one. One of the advantages of Box–Behnken design (BBD) is that they are all spherical design, the sample combinations are processed such that they are located at mid points of edges constituted by any two factors and require factors to be run at only of three levels that is represented by $[-1,0,1]$ [28]. The three examined levels and experimental ranges of each independent variable are given in Table 1. The relationship between the variables and the response was calculated by the second order polynomial equation. The form of the full quadratic model is shown in Eq. (4) as follows:

$$Y = \beta_0 + \sum \beta_i x_i + \sum \beta_{ii} x_i^2 + \sum \beta_{ij} x_i x_j \quad (4)$$

where Y is the predicted response or output (dependent variable), x_i and x_{ij} are the coded independent variables, β_0 is the intercept term, β_i the linear effect (first order), β_{ii} the squared effect, and β_{ij} is the interaction effect, i and j are the index numbers for variables.

Experimental design and data analysis were performed by using the Design of Experiment software (trial version 10).

3. Results and discussion

3.1. Catalysts characterization

The XRD patterns of the support ($\gamma-Al_2O_3$), V_2O_5 and $V_2O_5/\gamma-Al_2O_3$ with different loading of 5 wt%, 10wt%, 15wt% and 20 wt% after calcinations are shown in Fig. 2. The $\gamma-Al_2O_3$

characteristic peaks appeared at 45.8, 67 and 37.6° (JCPDS 10-425) (Fig. 2a). For reference, the diffractogram of pure V₂O₅ is also showed. The peaks located at 2θ = 20.52°, 21.96°, 26.39° and 31.30° can be assigned to the (0 1 0), (1 1 0), (1 0 1) and (4 0 0) planes of V₂O₅, respectively (Fig. 2b). All of the diffraction peaks of V₂O₅ are not distinct when its loading is lower than 15 wt. % but for higher than 15 wt. %, the diffraction peaks appear (Fig. 2e) and their intensity increases with the V₂O₅ loading, which is attributing to formation of a crystalline aluminum vanadium oxide (V₂O₅/γ-Al₂O₃) phase (Fig. 2f). The average crystallite size of (20 wt %) V₂O₅/γ-Al₂O₃ sample determined from the diffraction peak broadening by using the Scherer's formula was 22.4 nm (Fig. 2f). For the 15 wt% catalyst obtained some low intense broad peaks which confirmed the lowest crystallinity of V₂O₅/γ-Al₂O₃ catalysts and high dispersion of V₂O₅ particles on the support surface.

In addition, the SEM images (Fig. 3) of the pure γ-Al₂O₃, V₂O₅ and V₂O₅ (15wt %) / γ-Al₂O₃ sample indicated that agglomerated spherical vanadium oxides particles were well deposited on the surface of γ-Al₂O₃. According to Fig. 3f the particle sizes of V₂O₅ (15wt %) / Al₂O₃ sample was within the range of 17-35 nm.

NH₃-TPD profiles of V₂O₅/γ-Al₂O₃ catalysts with different V₂O₅ loadings are shown in Fig. 4. For γ-Al₂O₃ support, three desorption steps can be observed, which represent weak acidic sites (77–300°C), medium acidic sites (300–450°C) and strong acidic sites (450–600°C), respectively. These profiles were deconvoluted with the Gaussian curve fitting method, with results reported in Table 2. As observed in Fig.4, by increasing the amount of V₂O₅ on the γ-Al₂O₃ from 0wt% to 20wt%, the number of weak-medium acid sites continuously increased which implies that the addition of vanadium could cover strong acidic sites. Therefore, it seems that by increasing the V₂O₅ loading, the peaks of strong-strength acid sites shifted to low temperatures. The results are summarized in Table 2,

(area of the peaks at the low temperature was larger than the peaks at the high temperature).

In many studies have been reported that deactivation is related to the acid sites strength. Therefore, high strength sites may be leading reactions to produce heavy products which deposited on the catalyst surface. Their catalytic results showed a straight forward relationship between amount of V_2O_5 and weak moderate acidic properties. This behavior could be inferred from the shift of the acid sites distribution toward lower desorption temperatures, as observed in the corresponding NH_3 -TPD curves [29].

Several catalytic systems reported that Brønsted acid sites with combination of weak-medium acid strength have important influences on reaction performance and improve acrolein selectivity in the glycerol transformation [30-32]. Therefore pyridine adsorption coupled to FTIR analysis were taken to evaluate the nature of acidic sites. The spectra of pyridine adsorbed γ - Al_2O_3 and V_2O_5/γ - Al_2O_3 catalysts with different amount of V_2O_5 after out gassing at 100 °C are shown in Fig. 5(a-e). Lewis and Brønsted acid sites were identified by two bands at around 1450, 1610 cm^{-1} (attributing to the absorptions of pyridine on the Lewis acid centers) and 1545, 1637 cm^{-1} (attributing to pyridine coordinated to Brønsted acid sites). Furthermore, the band at about 1495 cm^{-1} attributed to combination of both Brønsted and Lewis (B+L) acid sites [12, 29 and 33]. These results demonstrate that the γ - Al_2O_3 support had only Lewis acid sites and the total acidity of bare γ - Al_2O_3 was 1.288 mmol $NH_3/g.cat$ (Table 2). However spectra for the V_2O_5 on the γ - Al_2O_3 catalysts showed the presence of both Brønsted and Lewis acid sites. As shown in Table 2, the 15wt% V_2O_5/γ - Al_2O_3 catalyst had the highest Brønsted sites concentration and then dramatically decreased at higher loading of vanadium (20 wt% V_2O_5/γ - Al_2O_3), which is maybe due to decrease in surface area and low dispersion of the active sites because of the agglomeration of vanadium species and also their interval diffusion

limitations which enhanced the coke formation [14, 27]. The specific surface area, pore structure property and vanadium oxide surface density for $V_2O_5/\gamma-Al_2O_3$ catalysts of this study are tabulated in Table 3. It is apparent that by increasing of V_2O_5 loading, BET surface areas are gradually decreased from $230\text{ m}^2\text{g}^{-1}$ with average pore volume of $0.28\text{ cm}^3\text{g}^{-1}$ to $168\text{ m}^2\text{g}^{-1}$ with average pore volume of $0.20\text{ cm}^3\text{g}^{-1}$, indicating that penetration of surface vanadium species into the pores of gamma alumina. This feature was confirmed by the pore size distribution, which shows the existence of pores ranging between 7 to 6.2 nm and consistent with previous report that vanadium species tend to have a strong interaction with the $\gamma-Al_2O_3$ support.

The temperature programmed reduction (TPR) of supported V_2O_5 (with different amount of vanadium oxides from 5 to 20 wt.%) were performed to evaluate the reducibility of catalysts, (Fig. 6 a-d). According to the literature [34-36] three peaks at approximately $350-420\text{ }^\circ\text{C}$, $480-550\text{ }^\circ\text{C}$ and $650-720\text{ }^\circ\text{C}$, are attributed to isolated vanadium species (with highly dispersion), polymeric vanadium species and bulk-like V_2O_5 , respectively. As can be seen, by increasing of V_2O_5 loadings from 5.0 to 15.0 wt%, the reduction temperature of the supported V_2O_5 catalysts shifted to higher temperature, This is mainly because of polymeric vanadium species deposited on the support that might be more difficult to reduce than isolated vanadium species under the TPR conditions or significant interaction between V_2O_5 and $\gamma-Al_2O_3$ support along with the formation of crystalline phases of V_2O_5 . The existence of a shoulder for 15 wt.% $V_2O_5/\gamma-Al_2O_3$ is attributed to the reduction of the highly dispersed vanadium species gradually from V^{5+} to V^{4+} and V^{4+} to V^{3+} [37]. However, by increasing of V_2O_5 content, the reduction peak area at $700\text{ }^\circ\text{C}$ was markedly increased due to high concentration of crystalline phases of V_2O_5 . This clearly suggests that the high V_2O_5 content sample (20 wt.% $V_2O_5/\gamma-Al_2O_3$) has more amounts of reducible V^{5+} species, which is also confirmed by X-ray diffraction pattern, Fig.2 f.

3.2. Analysis of data and Development of the response surface model

In the Box-Behnken design, 17-experimental observations were undertaken at random orders for the optimization of glycerol conversion (%) and acrolein selectivity (%) in the dehydration reaction and then the yield of acrolein was determined. Table 4 shows the data resulting from the effect of three variables: temperature (A), V_2O_5 (wt. %) loading on the support (B) and gas hourly speed velocity (G.H.S.V) (C), while the other factors are constant.

Analysis of variances (ANOVA) was used to evaluate the effects of main factors and their interactions. The results of the second order response surface model fitting in the form ANOVA for glycerol conversion and acrolein selectivity are shown in Tables 5 and 6 respectively. The 'Pred R-Squared' of 0.9835 is in reasonable agreement with the 'Adj R-Squared' of 0.9948. 'Adeq Precision' measures the signal to noise ratio. The ratio of 46.515 indicates an adequate signal and this model can be used to navigate the design space. The Model F-value of 340.06 implies that the model is significant. There is only a 0.01% chance that a 'Model F-value' this large could occur due to noise. The large value of F indicates that the most of the variation in the response can be explained by the regression equation. Values of 'Prob> F' less than 0.0500 indicate that the model terms are significant. In this case A, B, C, AB, AC, BC, A^2 , B^2 , C^2 are significant model terms. The Lack of Fit F-value of 2.28 implies that the Lack of Fit is not significant relative to the pure error. There is a 22.12% chance that a Lack of Fit F-value this large could occur due to noise (non-significant lack of fit is good). A quadratic model with statistical significance from a combination of estimates for the variables and the ANOVA results can be produced. The quadratic model was used to explain the mathematical

relationship between the independent variables and dependent responses which are represented by Eq. (5, 6).

$$\text{GLY Conv(\%)} = 94.30 + 9.83A + 7.59B - 14.05C + 8.51AB - 8.19AC - 0.59BC - 15.03A^2 - 14.09B^2 - 9.11C^2 \quad (5)$$

$$\text{ACR sele(\%)} = 71.67 - 9.33A + 7.84B + 2.90C - 4.68AB + 0.45AC + 0.58BC - 22.32A^2 - 20.36B^2 - 0.24C^2 \quad (6)$$

A positive sign before a term indicates a synergistic effect, while a negative sign indicates an antagonistic effect [2, 28]. The presence of the significant XX cross terms in the model confirms that response depends on both single and mixture variables. According to the Eqs. 5 and 6 the binary terms indicates that there is a synergistic effect between temperature (A) and loading of V₂O₅ (B) for conversion of glycerol and there are two synergistic effects between other variables (BC and AC) for selectivity of acrolein, whereas an antagonistic effect resulted between V₂O₅ loading and reaction temperatures. The comparison between experimental and predicted values of response variables GLY Conv(%) and ACR Sele(%) are shown in Fig. 7. A line of unit slope, corresponding to zero error between actual and predicted values is also presented. The determination coefficients of the R² (0.9977 and 0.9955) were also high, indicating that the predicted results are matching satisfactorily with the experimental values.

3.3. Effect of process variables on the conversion of glycerol and selectivity of acrolein

The main effects of factors (A, B, C) on conversion of glycerol (GLY) and selectivity of acrolein (ACR) have been evaluated. Each response surface was created by keeping one of three variables constant at their center points. Although the conversion of GLY and selectivity of ACR are significantly increased by simultaneous increasing amount of V₂O₅ on support, for higher than 15wt% of V₂O₅ loading, the selectivity of ACR decreased

dramatically. Other than the individual effect contributed by each main variable, the responses were also influenced by the interaction variables. In order to gain a better understanding of the interaction effects of variables on conversion and selectivity, 3D surface plot for the measured responses were formed based on the model equations (Eq. 5-6). The resulted surface response 3-D plots of GLY conversion and ACR selectivity as a function of two independent variables, (a, d) loading of V_2O_5 on the $\gamma-Al_2O_3$ and temperature; (b, e) G.H.S.V and temperature; (c, f) loading of V_2O_5 on the $\gamma-Al_2O_3$ and G.H.S.V are shown in Fig. 8(a)-(f), respectively.

As can be seen in Fig.8, Temperature had a different effect on the conversion of GLY and selectivity of ACR. The conversion of glycerol is significantly increased by simultaneous increasing of temperature (A), while it seems that optimum temperature for ACR selectivity is lower than 300 °C, Fig.8 (a, b and d, e). When the loading of V_2O_5 on $\gamma-Al_2O_3$ increases from 5 wt% to 15wt%, selectivity of ACR will increase because there are more Brønsted acid sites available for the reaction mechanism leading to the production of ACR. Fig. 8(c) shows that conversion of GLY decreases with increasing G.H.S.V from 120 to 540 h^{-1} and increases by increasing V_2O_5 loaded on support. At high level of G.H.S.V (540 h^{-1}) and middle level of V_2O_5 loading and low temperature maximum selectivity of ACR was obtained, while high level of catalyst and temperature and low level of G.H.S.V maximized GLY conversion. This simply means that the G.H.S.V and temperature are two factors which could be adjusted within the range to obtain a high yield of ACR. Thus, we can conclude that the yield of ACR is significantly increased by increasing of gas hourly space velocity, at constant V_2O_5 loading. In high temperatures the fast conversion leads to a high concentration of products and this might interfere by blocking the acidic sites, indicating that the selectivity of ACR is reduced considerably. Therefore, desorption rate of unwanted products is facilitated by increasing in G.H.S.V.

On the other hand, it seems to eliminate or slow down coke deposition on catalyst surface [38].

3.4. Validation of the experimental model

Response optimizer helps to identify the combination of input variable settings that jointly optimize a single response or a set of responses [28]. The software was used to predict the best conditions for the yield of acrolein (ACR) by pre-setting certain criteria, as shown in Table 7. The optimum values of the independent variables are obtained considering the lower and higher values of temperature, V_2O_5 loading and gas hourly space velocity (G.H.S.V). It was found that yield of higher than 68.31% for ACR could be achieved when using the V_2O_5 loading higher than 12.5 (wt%), the temperature of higher than 250 °C and the G.H.S.V lower than 540 h^{-1} . It was predicted that for amount of V_2O_5 on the γ - Al_2O_3 = 14.80wt% , G.H.SV of 268.60 h^{-1} and temperature = 286.35°C the yield of the ACR would be 73.05%, while the actual result for the maximum yield was 68.31% for 12.5 wt% loading of V_2O_5 on the γ - Al_2O_3 , G.H.S.V = 330 h^{-1} and reaction temperature of 285 °C. These results demonstrated that the predicted values are matching satisfactorily with the experimental ones. Therefore, obtained data from RSM technique, as mentioned above, let us to suggest the better operation conditions for dehydration reaction of glycerol (GLY) to acrolein (ACR).

3.5. Effect of reaction time

The effect of reaction time on catalytic activity of 12.5 wt% V_2O_5 / γ - Al_2O_3 at 285 °C is shown in Fig. 9. To evaluate the stability of catalyst, dehydration of glycerol was carried out under atmospheric pressure for 1, 3, 6 and 9 h under G.H.S.V of 330 h^{-1} . The reactor was fed with aqueous solution contained 30% (in mass) of glycerol at a feed flow rate of 2

mL.h⁻¹ by means of HPLC pump. According to Table 8, maximum glycerol conversion (99.28 %) can be achieved in the early hour (TOS 1h) and then gradually decreased by further increasing of reaction progress, which it is probably due to the high reactivity of acrolein, the side reactions and formation of larger molecules and coke formation, as previously mentioned [18]. For better understanding, The TG and DTA curves of spent catalyst after 3 and 9 h are shown in Fig.10. It can be seen from the TG curve that total weight loss for spent catalyst after 3 h is smaller than after 9 h. Furthermore, two exothermic peaks are appeared in the DTA curves. First peak is attributed to reoxidation of V⁴⁺ to V⁵⁺ species which take place at lower temperature (around 350 °C) and second peak is due to formation of poly-glycols or large molecules (around 500 °C), respectively [15, 16]. Also, a small peak around 220°C is due to decomposition of carbonaceous species after 9 h on the catalyst surface while, no carbon content was observed at 3 h of reaction progress, Fig 10 a. As expected, coke formation over the active sites was mainly responsible for decreasing acid site density and will result in catalyst deactivation during the reaction. Therefore, the highest acrolein yield (68.31%) was achieved after 3 h. The low selectivity is expected due to limited availability of active vanadium sites and consecutive reactions such as acrolein degradation or polymerization, which confirmed by above findings. Hence, the acrolein yield after 9 h (52.30%) is much lower than after 3 h. similarly to acrolein, the yield of other products such as acetol, acetaldehyde, allyl alcohol and acrylic acid was decreased dramatically after 9 h.

4. Conclusions

A response surface model, based on the Box-Benkhen technique, was developed to describe the conversion of glycerol, acrolein selectivity and yield in gas phase dehydration

reaction of glycerol. Temperature programmed desorption of ammonia (NH_3 -TPD) showed that the amount of strong acid sites decreased by increasing of V_2O_5 loading while number of total acid sites significantly increased. Temperature programmed reduction (H_2 -TPR) showed that the high V_2O_5 content sample (20 wt.% $\text{V}_2\text{O}_5/\gamma\text{-Al}_2\text{O}_3$) has more amounts of reducible V^{5+} species, which is mainly because of crystalline phase of V_2O_5 . The obtained results from ANOVA showed that the most significant factor affecting the conversion of GLY and ACR selectivity were gas hourly space velocity of carrier gas and reaction temperature, respectively. In addition, the interactions between temperature and V_2O_5 loading ($A \times B$), V_2O_5 loading had significant effects on the GLY conversion and ACR selectivity. Coefficient of determination (R^2) value of 0.9977 and 0.9958 obtained from Eqs. (5) and (6) shown that quadratic polynomial regression model could properly interpret the experimental data.

Also, we found that the catalytic activity and amount of Brønsted acid site depend on G.H.S.V and amount of V_2O_5 on the support and both are required for the high yield of ACR. The spent catalyst was also investigated by TG/DTA analysis and results showed that there is a significant decrease in the weight loss of the spent samples which leading to a decrease in the conversion and yield of acrolein after 9 h reaction. Thus, weak-medium strength acid sites efficiently promoted the dehydration reaction. With 14.80wt% of $\text{V}_2\text{O}_5/\gamma\text{-Al}_2\text{O}_3$, reaction temperature of 286.35°C and low level of G.H.S.V (268.60 h^{-1}), we could achieve the highest yield of acrolein (73.05%). Also, to show the validity of this prediction, we run the experiment at this condition and gained 68.31% for the yield of acrolein. These studies confirm that the predicted values are fully compatible with the experimental values.

Figure Captions

Fig.1. Continuous fixed-bed reactor applied for dehydration

Fig.2. XRD patterns of (a) γ -Al₂O₃, (b) V₂O₅, (c) (5wt %) V₂O₅/ γ -Al₂O₃, (d) (10 wt %) V₂O₅/ γ -Al₂O₃, (e) (15 wt %) V₂O₅/ γ -Al₂O₃ and (f) (20wt %) V₂O₅/ γ -Al₂O₃ calcined at 600 °C for 5 h.

Fig.3. SEM images of (a, b) V₂O₅, (c, d) V₂O₅ (15wt %) /Al₂O₃, (e) pure γ -Al₂O₃ and (f) V₂O₅ (15wt %) /Al₂O₃ along with particle sizes of V₂O₅ calcined at 600 °C for 5 h.

Fig.4. NH₃ desorption curves from NH₃-TPD over: (a) γ -Al₂O₃, (b) (5 wt %) V₂O₅/ γ -Al₂O₃, (c) (10wt %) V₂O₅/ γ -Al₂O₃, (d) (15 wt %) V₂O₅/ γ -Al₂O₃ and (e) (20 wt %) V₂O₅/ γ -Al₂O₃ calcined at 600 °C for 5 h.

Fig.5. FTIR spectra of pyridine adsorbed on: (a) pure γ -Al₂O₃, (b) (5 wt %) V₂O₅/ γ -Al₂O₃, (c) (10 wt %) V₂O₅/ γ -Al₂O₃, (d) (15 wt %) V₂O₅/ γ -Al₂O₃ and (e) (20 wt %) V₂O₅/ γ -Al₂O₃.

Fig.6. H₂-TPR profiles of (a) (5 wt %) V₂O₅/ γ -Al₂O₃, (b) (10 wt %) V₂O₅/ γ -Al₂O₃, (c) (15 wt %) V₂O₅/ γ -Al₂O₃ and (d) (20 wt %) V₂O₅/ γ -Al₂O₃.

Fig.7. Comparison between experimental and predicted values. *Small*: for GLY conversion. *Large*: for ACR selectivity.

Fig.8. 3D surface plots describing the response surface for: (*Left*: GLY conversion, *Right*: ACR selectivity) as function of:

(a,d) Loading of V₂O₅/ γ -Al₂O₃ vs. temperature at G.H.S.V= 330h⁻¹.

(b,e) G.H.S.V vs. temperature at loading of V₂O₅/ γ -Al₂O₃= 12.5 wt%.

(c,f) G.H.S.V vs. Loading of $V_2O_5/\gamma-Al_2O_3$ at temperature = 285 °C.

Fig .9. Glycerol conversion and acrolein selectivity and yield over 12.5 wt% $V_2O_5/\gamma-Al_2O_3$ with time.

Fig .10. TG and DTA curves of the spent 12.5 wt% $V_2O_5/\gamma-Al_2O_3$ catalyst after 3 and 9 h of reaction.

References

- [1] B. Katryniok, S.B Paul, F. Dumeignil, *ACS Catal.*, 2013, **3**, 1819.
- [2] A. Talebian-Kiakalaieh, N.A.S Amin, *Ind. Eng. Chem. Res.*, 2015, **54**, 8113.
- [3] X. Feng, Y.Yao, Q. Sua, L. Zhaoa, W. Jianga and W. Ji, *Appl. Catal., B*, 2015, **164**, 31.
- [4] M.M. Bettahar, G. Costentin, L. Savary and J.C. Lavalley, *Appl. Catal., A*, 1996, **145**, 1.
- [5] Z. Wang, L.Wang, Y. Jiang, M. Hunger and J. Huang, *ACS Catal.*, 2014, **4**, 1144.
- [6] D. Stosic, S. Bennici, S. Sirotin, P. Stelmachowski, J. Couturier, J. Dubois, A. Travert and A. Auroux, *Catal. Today*, 2014, **226**, 167.
- [7] L. Shen, H. Yin, A. Wang, Y. Feng, Y. Shen, Z. Wu and T. Jiang, *Chem.Eng. J.*, 2012, **180**, 277.
- [8] W. Yan, G.J. Suppes, *Ind. Eng. Chem. Res.*, 2009, **48**, 3279.
- [9] L. Shen, H. Yin, A. Wang, X. Lu and C. Zhang, *Chem. Eng. J.*, 2014, **244**, 168.
- [10] A. S. de Oliveira, S.J.S.Vasconcelos, J.R. de Sousa, F.F. de Sousa, J.M. Filho and A.C. Oliveira, *Chem. Eng. J.*, 2011, **168**, 765.
- [11] L. G. Possato, R. N. Diniz, T. Garetto, S. H. Pulcinelli, C. V. Santilli and L. A Martins, *J. Catal.*, 2013, **300**, 102.
- [12] R. Estevez, S. Lopez-Pedrajas, F. Blanco-Bonilla, D. Luna and F.M. Bautista, *Chem. Eng. J.*, 2015, **282**, 179.
- [13] J.L. Dubois, C. Duquenne, W. Holderich, Arkema FR 2884818 or WO2006087083 A2 2006.
- [14] A. Talebian-Kiakalaieh, N.A.S. Amin, H. Hezaveh, *Renew. Sust. Energy Rev.*, 2014, **40**, 28.
- [15] F.Wang, J.L. Dubois, W. Ueda, *Appl. Catal., A*, 2010, **376**, 25.

- [16] F. Wang, J.Ldubois, W. Ueda, *J. Catal.*, 2009, **268**, 260.
- [17] Y. Kamiya, H. Nishiyama, M. Yashiro, A. Satsuma and T. Hattori, *J. Jpn. Pet. Inst.*, 2003, **46**, 62.
- [18] J.A. Cecilia, C. García-Sancho, J.M. Mérida-Robles, J. Santamaría-González, R. Moreno-Tost and P. Maireles-Torres, *Catal. Today*, 2015, **254**, 43.
- [19] A. Alhanash, E. F. Kozhevnikova, I. V. Kozhevnikov, *Appl. Catal., A*, 2010, **378**, 11.
- [20] A. Chierigato, M. Dolores Soriano, E. Garcia-Gonzalez, G. Puglia, F. Basile, P. Concepcion, C. Bandinelli, J. M. Lopez Nieto and F. Cavani, *Chem.Sus.Chem*, 2015, **8**, 398.
- [21] A. Chierigato, C. Bandinelli, P. Concepcion, M. D. Soriano, F. Puzzo, F. Basile, F. Cavani and J. M. Lopez Nieto, *Chem.Sus.Chem*, 2016, **9**, 1.
- [22] P. J. Souza, Th. Melo, M.A.L. de Oliveira, R.M. Paniago, P.P. de Souza and L.C.A. Oliveira, *Appl. Catal., A*, 2012, **443**, 153.
- [23] J.L. Dubois, C. Duquenne, W. Holderich and J. Kervennal, Arkema FR 2882053 A1 or US2008214880 A1 2006.
- [24] K. Omata, S. Izumi, T. Murayama and W. Ueda, *Catal. Today*, 2013, **201**, 7.
- [25] K.M. Parida, A.C. Pradhan, J. D. Nruparaj Sahu, *Mater. Chem. Phys.*, 2009, **113**, 244.
- [26] A. Pan, J.G. Zhang, Z. Nie, G. Cao, B. W. Arey, G. Li, Sh. Liang and J. Liu, *J. Mater. Chem.*, 2010, **20**, 9193.
- [27] X. Hu, C. Li, C. Yang, *Catal. Today*, 2010, **158**, 504.
- [28] V. Mahdavi, A. Monajemi, *J. Taiwan Inst. Chem. Eng.*, 2014, **45**, 2286.
- [29] C. García-Sancho, J.A. Cecilia, A. Moreno-Ruiz, J.M. Mérida-Robles, J. Santamaría-González, R. Moreno-Tost, P. Maireles-Torres, *Appl. Catal. B*, 2015, **179**, 139.
- [30] B. Katryniok, S. Paul, V. Bellière-Baca, P. Reye and F. Dumeignil, *Green Chem.*, 2010, **12**, 2079.

- [31] A. Talebian-Kiakalaieh, N.A.S. Amin, *J. Taiwan Inst. Chem. Eng.*, 2016, **59**, 11.
- [32] N. PethanRajan, G. Srinivasa Rao, B.Putrakumar, K.V. R. Chary, *RSC Adv.*, 2014, **4**, 53419.
- [33] N. P. Rajan, G. Srinivasa Rao, V. Pavankumar and K. V. R. Chary, *Catal. Sci. Technol.*, 2014, **4**, 81.
- [34] M. Banares, J. Cardoso, F. Agulló Rueda, J. Correa Bueno and J. Fierro, *Catal. Lett.* 64 (2000) 191-196.
- [35] A. Held, J. Kowalska-Kuś and K. Nowińska, *Catal. Commun.* 17 (2012) 108-113.
- [36] B. Solsona, T. Blasco, J. L. Nieto, M. Pena, F. Rey and A. Vidal- Moya, *J. Catal.* 203 (2001) 443-452.
- [37] S. Besselmann, C. Freitag, O. Hinrichsen and M. Muhler, *Phys.Chem. Chem. Phys.*, 2001, **3**, 4633.
- [38] A. Talebian-Kiakalaieh, N.A.S. Amin, Z.Y. Zakaria, *J. Ind. Eng. Chem.*, 2016, **34**, 300.

Table 1

Experimental range and levels for Box-Behnken design

Independent variables	Range and level		
	-1	0	1
Temperature (°C), A	250	285	320
Loading V ₂ O ₅ (wt.%), B	5	12.5	20
G.H.S.V(h ⁻¹), C	120	330	540

Table 2Acid distribution of $V_2O_5/\gamma\text{-Al}_2\text{O}_3$ catalysts

Sample	Weak acid (mmol NH_3 g^{-1})	Middle acid (mmol NH_3 g^{-1})	Strong acid (mmol NH_3 g^{-1})	Total (mmol NH_3 g^{-1})	Brønsted sites/Lewis sites ^a
$\gamma\text{-Al}_2\text{O}_3$	0.715	0.310	0.263	1.288	0.0
5 $V_2O_5/\gamma\text{-Al}_2O_3$	0.810	0.322	0.213	1.345	0.31
10 $V_2O_5/\gamma\text{-Al}_2O_3$	0.908	0.330	0.182	1.420	0.55
15 $V_2O_5/\gamma\text{-Al}_2O_3$	0.985	0.395	0.099	1.479	0.89
20 $V_2O_5/\gamma\text{-Al}_2O_3$	1.023	0.464	0.059	1.546	0.63

^aRatio of the concentration of Brønsted and Lewis acid sites calculated from the adsorption of pyridine evacuated at 100°C.

Table 3

Texture properties of $V_2O_5/\gamma\text{-Al}_2\text{O}_3$ and vanadium surface density (V/nm^2) of catalysts after calcination at 600 °C.

Sample	Surface area (m^2/g)	Average pore volume (cm^3/g)	Average pore size (nm)	Surface density (V/nm^2)
$\gamma\text{-Al}_2\text{O}_3$	230	0.28	7.0	0
$5V_2O_5/\gamma\text{-Al}_2\text{O}_3$	222.5	0.26	6.8	1.7
$10V_2O_5/\gamma\text{-Al}_2\text{O}_3$	198	0.26	6.4	3.6
$15V_2O_5/\gamma\text{-Al}_2\text{O}_3$	190.5	0.24	6.4	5.9
$20V_2O_5/\gamma\text{-Al}_2\text{O}_3$	168	0.20	6.2	8

Table 4

Box-Behnken design matrix and results of the glycerol conversion, acrolein selectivity and yield.

Run	Temperature (°C)	Loading of V ₂ O ₅ (wt. %)	G.H.S.V (h ⁻¹)	Glycerol Conversion (%)		Acrolein Selectivity (%), (Yield) (%)*	
				Experimental	Predicted	Experimental	Predicted
1	320.0	20.00	330	90.15	91.11	22.18(20.01)	22.82(20.79)
2	285.0	20.00	540	55.14	54.05	63.88(35.29)	62.39(33.72)
3	285.0	12.50	330	92.45	94.30	71.15(65.77)	71.67(67.58)
4	285.0	12.50	330	94.03	94.30	72.65(68.31)	71.67 (67.58)
5	285.0	20.00	120	83.26	83.33	54.30(45.21)	55.43(46.18)
6	250.0	20.00	330	54.37	54.43	51.11(27.78)	50.84(27.67)
7	285.0	12.50	330	95.78	94.30	71.13(66.12)	71.67(67.58)
8	250.0	5.00	330	57.23	56.27	26.44(15.13)	25.80(14.51)
9	320.0	12.50	540	47.63	47.75	42.28(20.14)	43.13(20.59)
10	320.0	5.00	330	58.98	58.91	16.24(9.57)	16.50(9.72)
11	285.0	12.50	330	93.22	94.30	69.31(64.61)	71.67 (67.58)
12	250.0	12.50	540	43.44	44.47	59.14(25.69)	60.89(27.07)
13	285.0	5.00	120	65.89	66.97	39.42(25.98)	40.91(27.39)
14	250.0	12.50	120	56.31	56.19	56.85(32.05)	55.99(31.46)
15	285.0	5.00	540	40.11	40.05	46.69(18.72)	45.55(18.24)
16	320.0	12.50	120	93.25	92.23	38.19(35.61)	36.43(33.60)
17	285.0	12.50	330	95.03	94.30	71.50(67.94)	71.67 (67.58)

* Numbers in bracket related to yield of Acrolein.

Table 5

ANOVA of the model for the conversion of glycerol aqueous solution from Box-Behnken.

Source	Sum of Squares	df	Mean Square	F- Value	p-value Prob> F	
Model	7078.46	9	786.50	340.06	< 0.0001	significant
A	773.42	1	773.42	334.41	< 0.0001	
B	460.71	1	460.71	199.20	< 0.0001	
C	1578.94	1	1578.94	682.70	< 0.0001	
AB	289.51	1	289.51	125.18	< 0.0001	
AC	268.14	1	268.14	115.94	< 0.0001	
BC	1.37	1	1.37	0.59	0.4669	
A ²	951.29	1	951.29	411.31	< 0.0001	
B ²	835.73	1	835.73	361.35	< 0.0001	
C ²	1538.21	1	1538.21	665.09	< 0.0001	
Residual	16.19	7	2.31			
Lack of Fit	6.34	3	2.11	0.86	0.5309	not significant
Pure Error	9.85	4	2.46			
Cor Total	7094.65	16				

R-squared = 0.9977, Adj R-squared = 0.9948, Pred R-squared = 0.9835, Adeq precision = 46.515

Table 6

ANOVA of the model for the selectivity of acrolein from Box-Behnken

Source	Sum of Squares	df	Mean Square	F- Value	p-value Prob> F	
Model	5428.54	9	603.17	170.84	< 0.0001	significant
A	696.58	1	696.58	197.29	< 0.0001	
B	491.10	1	491.10	139.09	< 0.0001	
C	67.45	1	67.45	19.10	0.0033	
AB	87.70	1	87.70	24.84	0.0016	
AC	0.81	1	0.81	0.23	0.6466	
BC	1.33	1	1.33	0.38	0.5582	
A ²	2096.95	1	2096.95	593.92	< 0.0001	
B ²	1745.22	1	1745.22	494.30	< 0.0001	
C ²	0.24	1	0.24	0.067	0.8036	
Residual	24.71	7	3.53			
Lack of Fit	15.60	3	5.20	2.28	0.2212	not significant
Pure Error	9.12	4	2.28			
Cor Total	5453.26	16				

R-squared = 0.9958, Adj R-squared = 0.9903, Pred R-squared = 0.9568, Adeq precision = 38.275

Table 7

The preset criteria for optimization of the maximum conversion, selectivity and yield.

Factor/response	Goal	Lower limit	Upper limit
Temperature (°C) A	In range	250	320
Loading of V ₂ O ₅ (wt. %) B	In range	5	20
G.H.S.V (h ⁻¹) C	In range	120	540
GLY conversion (%)	Maximize	40.11	95.03
ACR Selectivity (%)	Maximize	16.24	72.65
ACR yield (%)	Maximize	9.57	69.23

Composite desirability = 1.00000

Table 8Product distribution results of glycerol dehydration over 12.5wt% V₂O₅/γ-Al₂O₃ catalyst

Time (h)	Conversion (%)	Yield (%)					
		acrolein	acetol	allyl alcohol	acetaldehyde	Acrylic acid	others
1	99.28	57.96	19.63	10.65	5.23	2.04	4.49
3	94.03	68.31	16.17	7.02	5.01	1.95	1.55
6	92.85	59.07	15.69	6.95	4.89	1.14	12.26
9	85.47	52.30	12.45	5.21	4.85	0.93	24.26

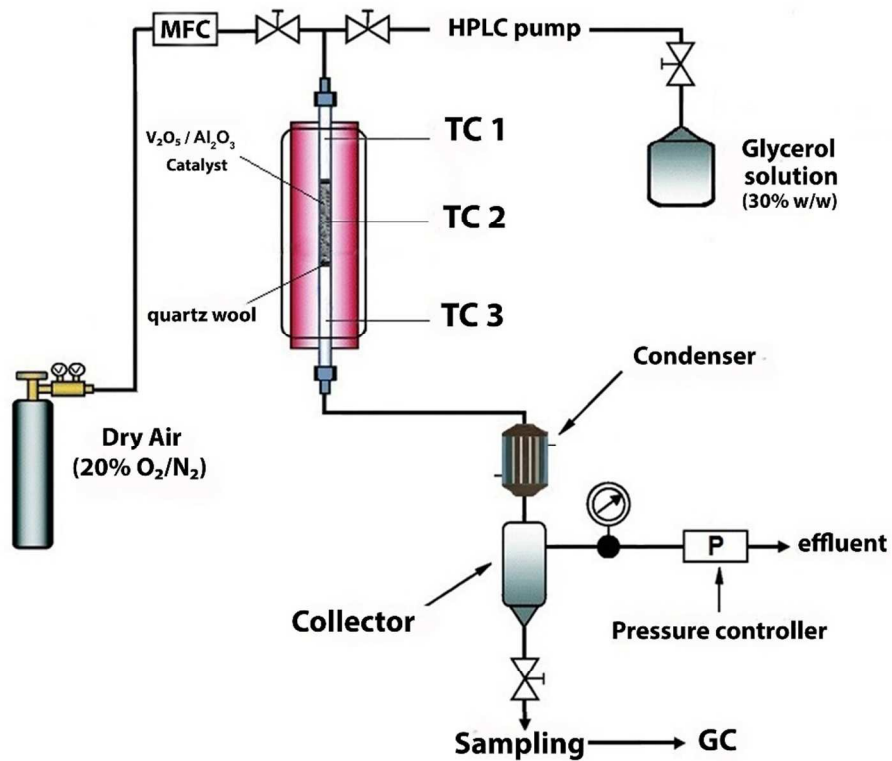


Fig 1

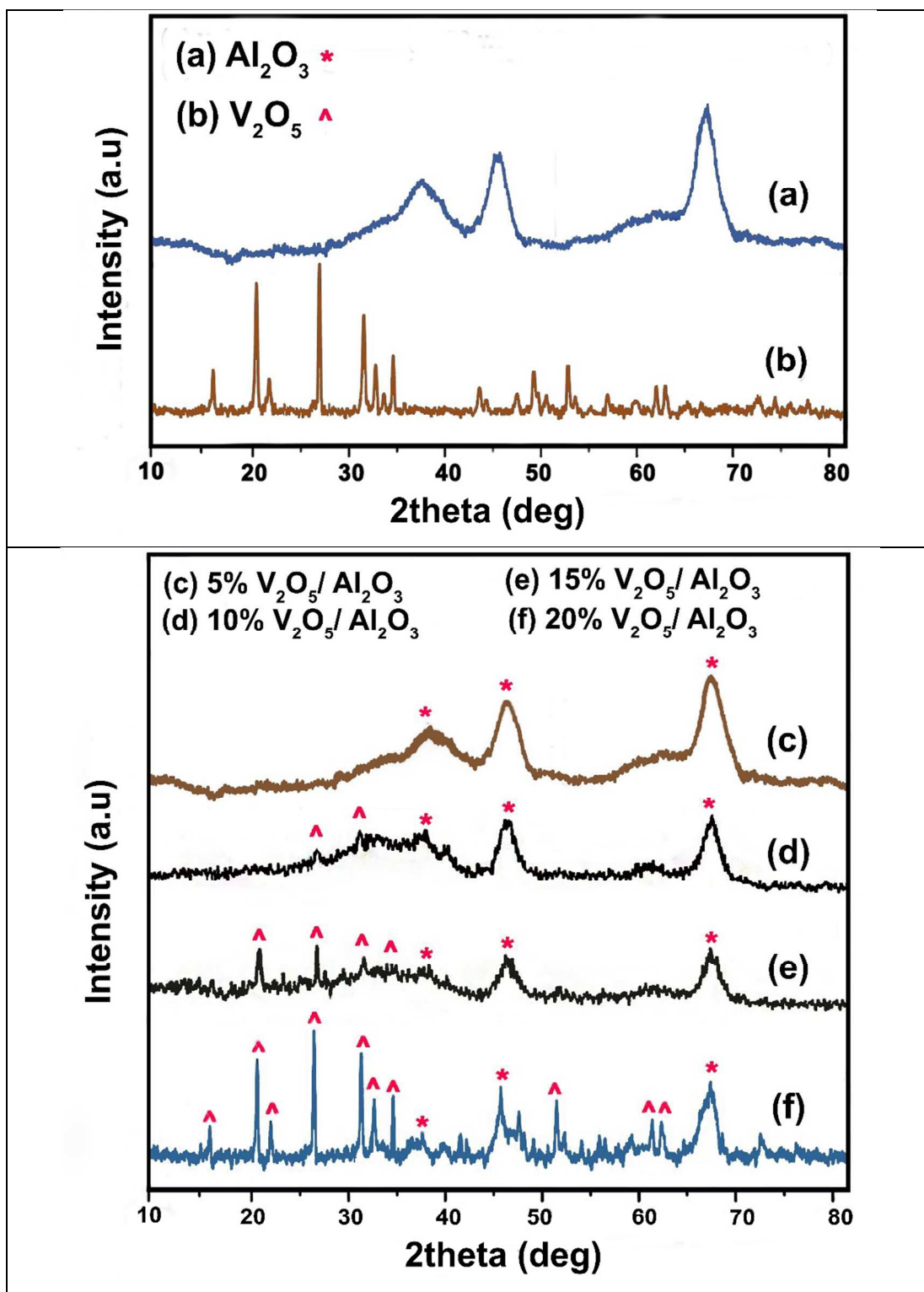


Fig 2

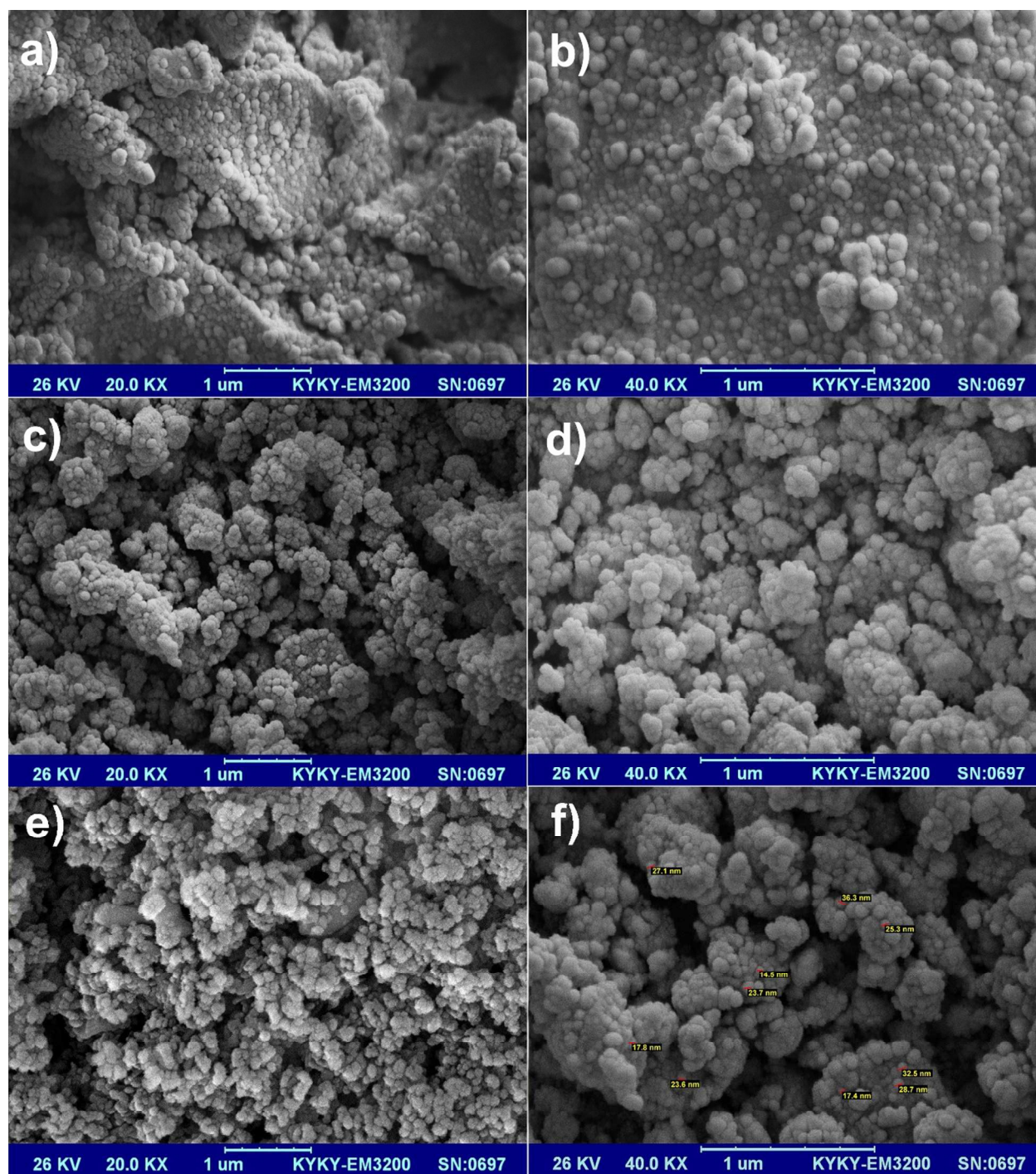


Fig 3

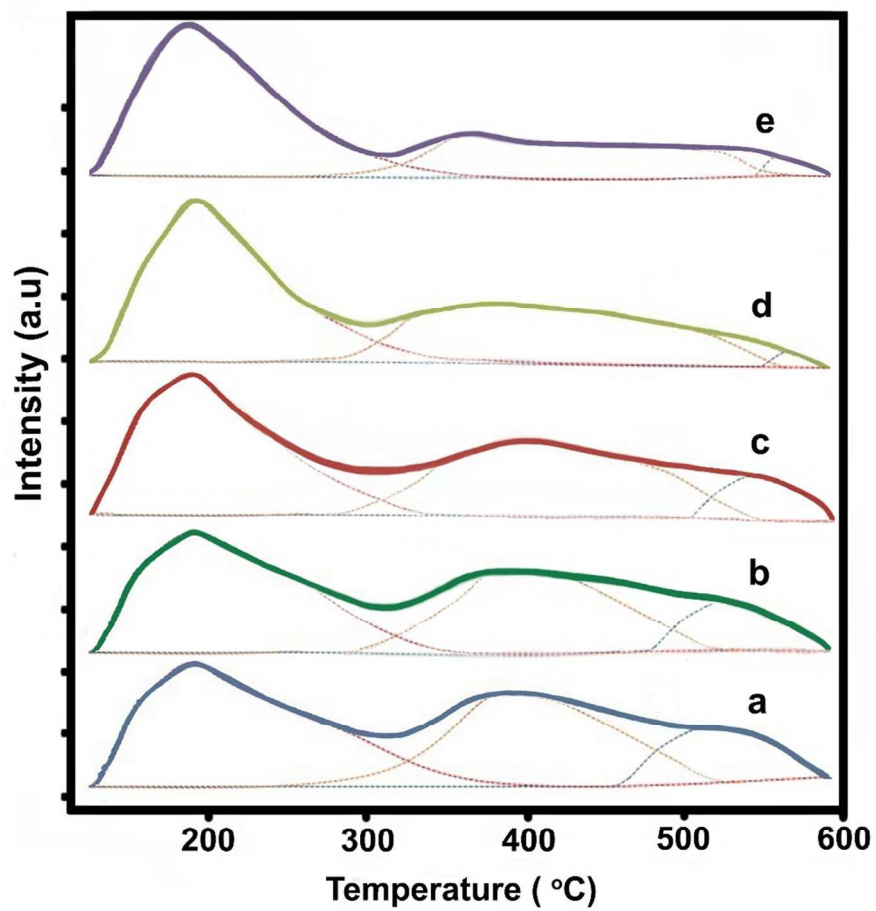


Fig 4

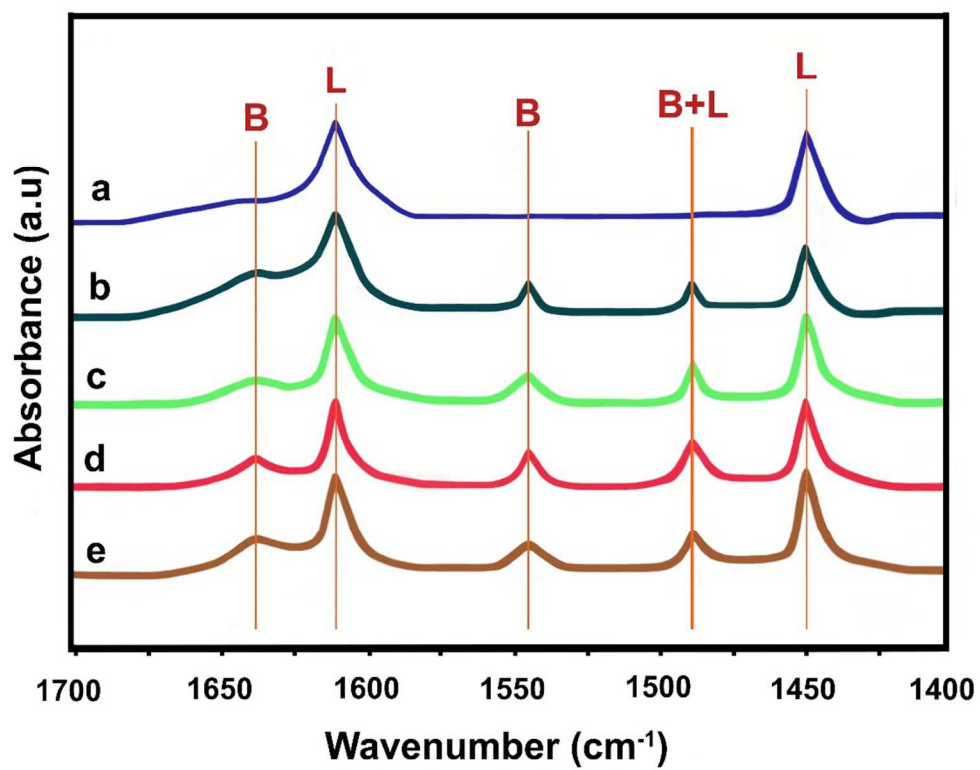


Fig 5

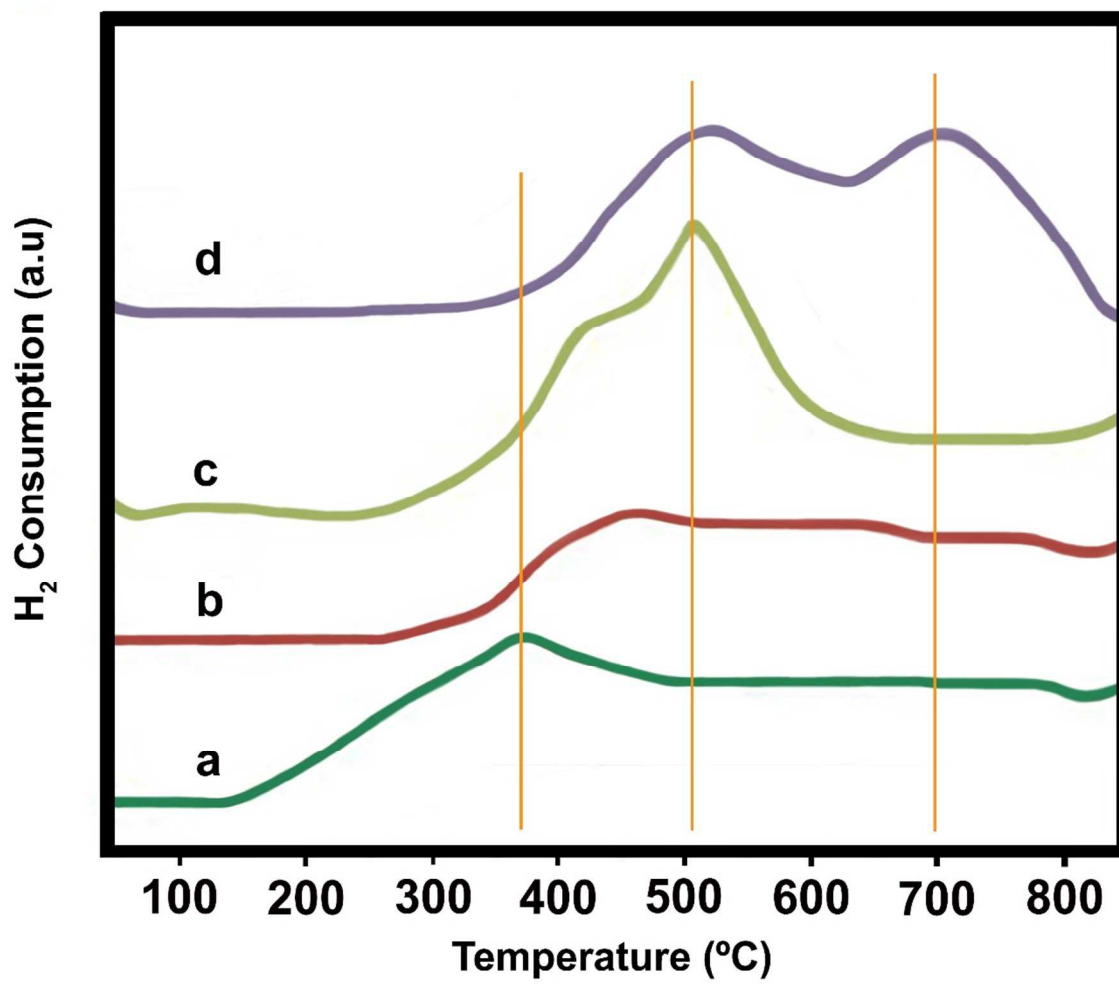


Fig 6

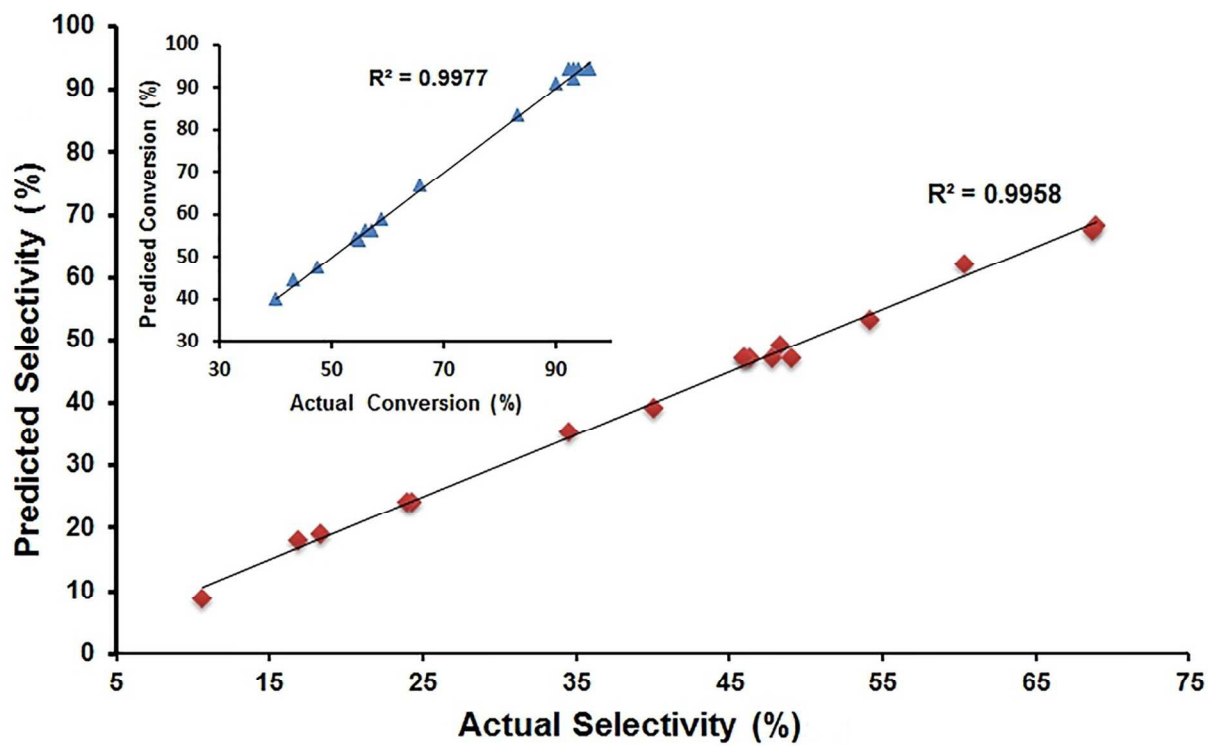


Fig 7

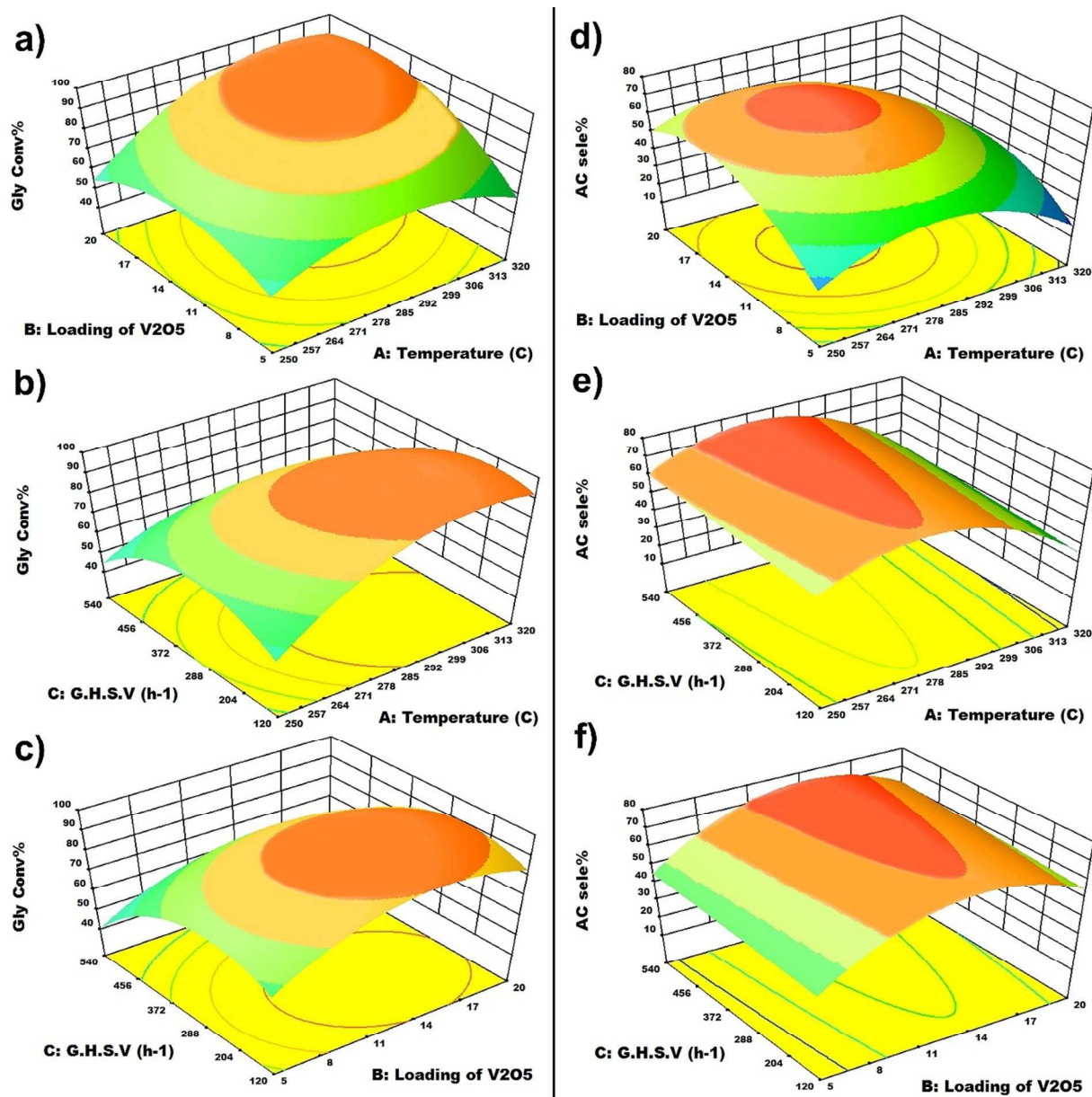


Fig 8

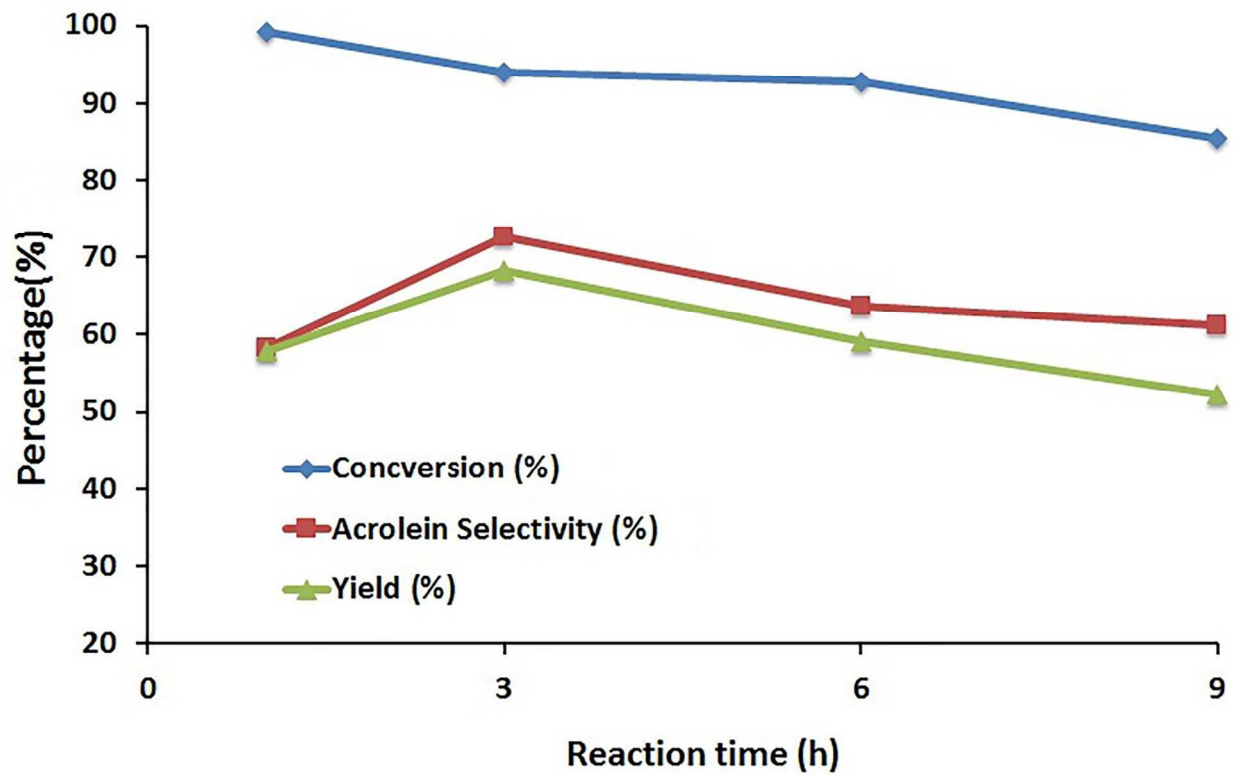


Fig 9

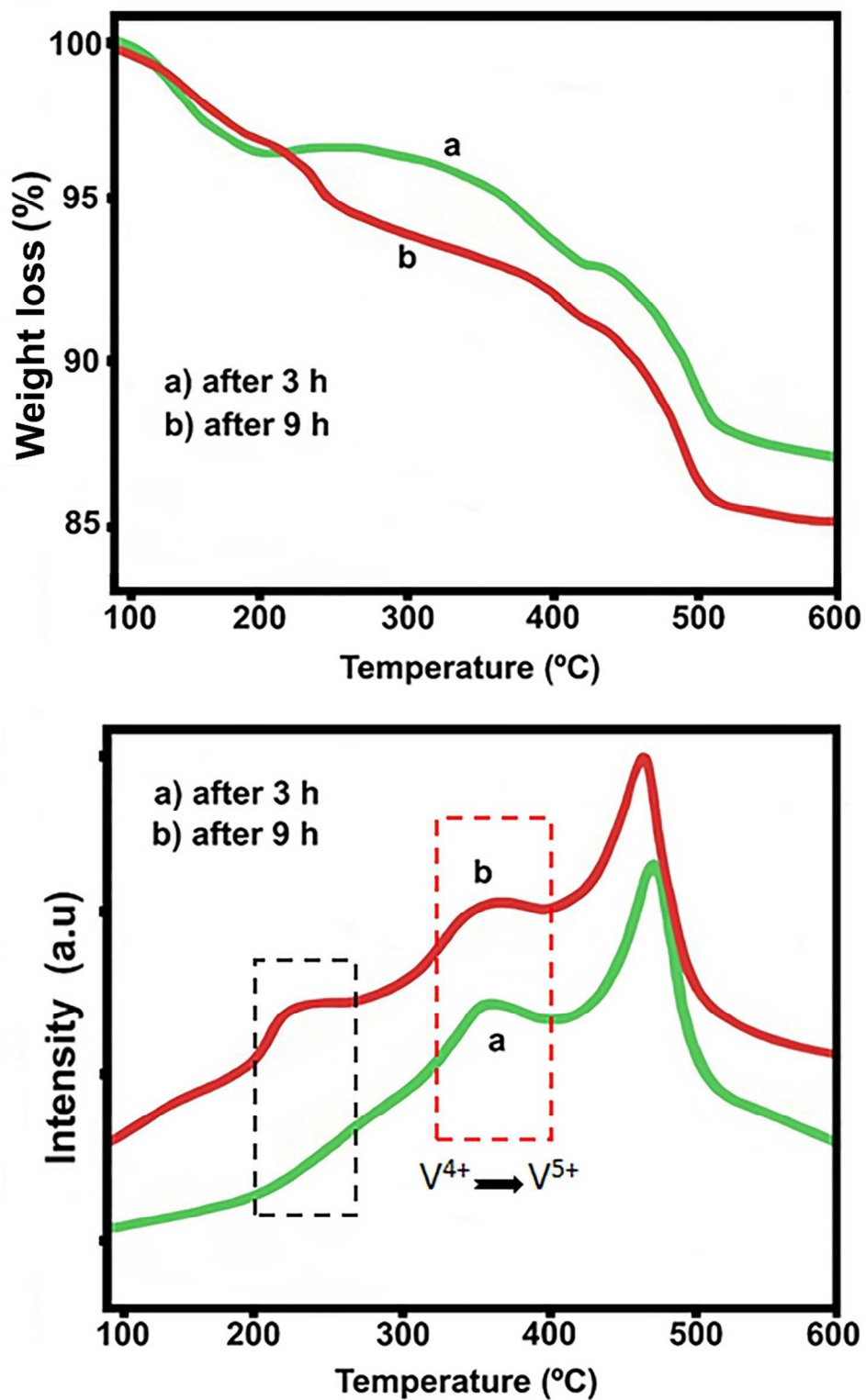


Fig 10

Graphical Abstract

